PHYSICAL REVIEW VOLUME 156, NUMBER 3 15 APRIL 1967

Vibrational Properties of Imperfect Crystals with Large Defect Concentrations

D. W. Taylor
Bell Telephone Laboratories, Murray Hill, New Jersey

(Received 14 November 1966)

The multiple-scattering theory of Lax is used to give equations for the displacement-displacement Green's functions for a crystal containing substitutional defect atoms. A self-consistent method is described within this formalism that is most suitable for large concentrations of mass defects. The essential approximation is best in three dimensions, but even then is not completely satisfactory for low concentrations of light defects. The resulting self-consistent equation is solved numerically using realistic three-dimensional densities of states. The behavior of the density of states and spectral functions for the imperfect crystal is discussed in some detail for different concentrations and mass ratios. The results are compared with recent machine calculations and found to be in good agreement. They are also used to reinterpret experimental results for Ge-Si alloys with some success.

1. INTRODUCTION

When an atom of different mass (mass defect) is added substitutionally to a crystal, its vibrational properties are considerably different from those of the atom it has replaced (host atom). If it is sufficiently light, it can cause a mode to split off the top of the vibrational continuum of the pure crystal to produce a local mode, so called because the amplitudes of the vibrations of this mode are strongly localized around the defect. A heavy defect prefers to vibrate at lower frequencies than the host atom, and, provided the defect is sufficiently heavy, this is seen as a low-frequency resonance in the response function. The changes in force constants that in general accompany a substitutional defect can have similar and more complicated effects. The techniques for calculating the behavior of such defects are well known and are described in a review article by Maradudin.[1]

When more than one defect is present they can interact giving a width to the local-mode frequency as well as producing additional modes attributable to adjacent defect pairs, triplets, etc. Langer[2] has given an approximate treatment of the density of states for small concentrations of mass defects in linear chains. The method is easily extended to three dimensions and it is reviewed, along with other work concerning small defect concentrations, in an article by Maradudin.[3] Elliott and Taylor[4] have recently discussed the same problem using double-time Green's functions[5] for the displacements. This is a particularly useful formalism as it leads very simply to the appropriate spectral functions required to discuss the density of states, optical absorption coefficient, and neutron scattering cross section in imperfect crystals. For the same reason we will use this formalism in this paper, also using the same notation where possible.

Although Elliott and Taylor were able to find a good measure of agreement between theory and experiment, there is one unsatisfactory feature of the theory. The spectral function in the local-mode region remains a delta function although the density of states has a finite width. This discrepancy led Davies and Langer[6] to propose a self-consistent procedure which we describe briefly in Sec. 4. This procedure still gives a small concentration result for reasons described in that section.

The most detailed descriptions of disordered crystals containing mass defects are given by the machine calculations of Dean and co-workers[7,8] for one and two dimensions and, more recently, by Payton and Visscher[9] for one, two, and three dimensions. Some of their results are given in Secs. 5 and 6 and provide an excellent test for approximate analytic theories.

These machine calculations are very time consuming, and it is of considerable interest to obtain an approximate analytic theory to describe disordered crystals at large defect concentrations. In this paper we give such a theory, which leads to a self-consistent equation that is not difficult to solve on a computer and whose solution is not very time consuming. The necessary approximation made in this method restricts its validity essentially to three dimensions.

We use the multiple-scattering formalism of Lax[10] which is described in Sec. 2 for the particular case at hand. The self-consistent method is described in Sec. 3 and a brief discussion of other self-consistent work is given in Sec. 4. The solution of the self-consistent equation, using a realistic density of states, is described in Sec. 5 and its behavior discussed in some detail. In Sec. 6 the solution is compared with the three-dimensional results of Payton and Visscher[9] with considerable success. It is also used to reinterpret the phonon-

---

[1] A. A. Maradudin, Rept. Progr. Phys. **28**, 331 (1965).

[2] J. S. Langer, J. Math. Phys. **2**, 584 (1961).

[3] A. A. Maradudin, Solid State Phys. **18**, 273 (1966).

[4] R. J. Elliott and D. W. Taylor Proc. Roy. Soc. (London) **A296**, 161 (1967) subsequently referred to as I.

[5] D. N. Zubarev, Usp. Fiz. Nauk SSSR [English transl.: Soviet Phys.—Usp. **3**, 320 (1960)].

[6] R. W. Davies and J. S. Langer, Phys. Rev. **131**, 163 (1963).

[7] P. Dean, Proc. Roy. Soc. (London) **A260**, 263 (1961).

[8] P. Dean and M. D. Bacon, Proc. Roy. Soc. (London) **A283**, 64 (1965).

[9] D. N. Payton and W. M. Visscher, Phys. Rev. **154**, 802 (1967).

[10] M. Lax, Rev. Mod. Phys. **23**, 287 (1951); Phys. Rev. **85**, 621 (1952).

assisted tunneling results in Ge-Si alloys of Logan, Rowell, and Trumbore[11] with some success.

The formalism for the vibrational properties of imperfect crystals is very similar to that used to describe the behavior of electrons in such crystals. Indeed Lax's formalism was given in terms of the electronic properties of random systems, and the methods extensively used by Beeby and Edwards[12] and more recently by Soven[13] are entirely equivalent to those of Lax. Recently Soven[14] has also described a self-consistent method for the electronic problem that is very similar in principle to the self-consistent method we describe in Sec. 3. Both these calculations are variants on a self-consistent procedure first suggested by Lax.[15]

An essential difference between our problem and the equivalent electronic problem that helps to make ours much more tractable lies in the form of the defect matrix or impurity potential. Even in three dimensions, a mass defect looks like a delta-function potential situated at a lattice site, whereas in order to give a realistic treatment for the electronic structure of α-brass, but without too much complexity, Soven[13] had to resort to delta-function shell potentials. In a self-consistent calculation for such a system both this form of potential and the reciprocal lattice vector summations (not present in the vibrational problem) must lead to equations of much more complicated nature as compared to our final equations (3.12) and (3.14).

Lifshitz[16] has recently given an extensive discussion of the systematics of the electron energy levels and the behavior of the band edges in disordered systems. In particular, he predicts that when the impurity potential is sufficiently different so as to split states off the bottom of the continuum, the edge of this continuum will move to higher energies as more of such impurities are added. When interpreted in terms of our problem this prediction is in agreement with our findings, as mentioned in Sec. 5.B.

2. GENERAL FORMULATION AND LOW-CONCENTRATION RESULT

The displacement-displacement double-time thermal Green's functions,[5] $G_{\alpha\beta}(l,l';\omega)$, are defined as

$$G_{\alpha\beta}(l,l';\omega)=\frac{1}{h}\int_{-\infty}^{\infty}\langle\langle u_\alpha(l,t);u_\beta(l',0)\rangle\rangle e^{i\omega t}dt\,, \qquad (2.1)$$

where

$$\langle\langle A(t);B(0)\rangle\rangle=i\theta(t-t')\langle[A(t),B(0)]\rangle\,,\quad\text{(retarded Green's functions)}$$
$$=-i\theta(t'-t)\langle[A(t),B(0)]\rangle\,,\quad\text{(advanced Green's function)}\,,$$
$$\theta(t)=1,\ t>0;\ =0,\ t<0.$$

The continuation of G into the upper (lower) half of the complex frequency plane gives the retarded (advanced) Green's functions. $u_\alpha(l,t)$ is the atomic displacement of the pth atom in the unit cell at $\mathbf{R}_l$ with Cartesian coordinate a, $\alpha=(a,p)$.

The correlation functions are given in terms of the spectral function $\mathcal{J}(\omega)$,

$$\langle A(t)B(0)\rangle=\int_{-\infty}^{\infty}e^{\beta\omega}\mathcal{J}(\omega)e^{-i\omega t}d\omega\,, \qquad (2.2)$$

where $\beta=h/k_BT$ at the temperature T. The spectral function is related to the Green's functions by

$$\mathcal{J}(\omega)=\frac{ih}{e^{\beta\omega}-1}\lim_{\varphi\to+0}[G(\omega+i\varphi)-G(\omega-i\varphi)]. \qquad (2.3)$$

The Hamiltonian for the imperfect crystal in the harmonic approximation is

$$\mathcal{H}=\tfrac{1}{2}\sum_{\alpha,l}\frac{p_\alpha^2(l,t)}{M_\alpha(l)}+\tfrac{1}{2}\sum_{\substack{\alpha\beta\\ ll'}}u_\alpha(l,t)\Phi_{\alpha\beta}(l,l')u_\beta(l',t)\,, \qquad (2.4)$$

where $M_\alpha(l)$ is the atomic mass and $\Phi_{\alpha\beta}(l,l')$ is the force-constant matrix. For a defect of type $\delta(l_i)$ at l_i, it is convenient to describe the change in mass,

$$M_\alpha-M_\alpha(l_i)=M_\alpha\epsilon_\alpha^{\delta(l_i)}\,, \qquad (2.5)$$

and the changes in the force constants from $\Phi_{\alpha\beta}^0(l,l')$ to $\Phi_{\alpha\beta}(l,l')$,

$$\Delta\Phi_{\alpha\beta}^{\delta(l_i)}(l,l')=\Phi_{\alpha\beta}(l,l')-\Phi_{\alpha\beta}^0(l,l')\,, \qquad (2.6)$$

by the defect matrix

$$C_{\alpha\beta}^{\delta(l_i)}(l,l';\omega)=\Delta\Phi_{\alpha\beta}^{\delta(l_i)}(l,l')+M_\alpha\epsilon_\alpha^{\delta(l_i)}\omega^2\delta_{\alpha\beta}\delta(l,l')\delta(l,l_i). \qquad (2.7)$$

By the equations-of-motion method, it can be shown (see Paper I) that the relation between the Green's function for the imperfect crystal, $\mathbf{G}$, and that for the perfect crystal, $\mathbf{P}$, is

$$\mathbf{G}(l,l';\omega)=\mathbf{P}(l,l';\omega)+\sum_{l_1l_2}\mathbf{P}(l,l_1;\omega)\mathbf{C}(l_1,l_2;\omega)\times\mathbf{G}(l_2,l';\omega)\,, \qquad (2.8)$$

where the total defect matrix is given by

$$\mathbf{C}(l,l';\omega)=\sum_i\mathbf{C}^{\delta(l_i)}(l,l';\omega). \qquad (2.9)$$

In general, forming the total defect matrix by the addition of independent individual defect matrices is only satisfactory at small defect concentrations. The

---

[11] R. A. Logan, J. M. Rowell, and F. A. Trumbore, Phys. Rev. **136**, A1751 (1964).

[12] S. F. Edwards, Proc. Roy. Soc. (London) **A267**, 518 (1962); S. F. Edwards and J. Beeby, *ibid.* **A274**, 395 (1962); J. Beeby, *ibid.* **A279**, 82 (1964).

[13] P. Soven, Phys. Rev. **151**, 539 (1966).

[14] P. Soven, this issue, Phys. Rev. **156**, 809 (1967).

[15] M. Lax (unpublished).

[16] I. M. Lifshitz, Advan. Phys. **13**, 483 (1964).

change of the force constant connecting two atoms depends, at least, upon whether they are both defect atoms, both host atoms, or one is a defect atom and the other is a host atom. In fact, it is quite conceivable that the change in force constant between two atoms can depend in a more complicated way upon the local environment of the two atoms. For short-range forces, the form of (2.7) and (2.9) will only be valid when the probability of two defect atoms being near each other is small, i.e., at small concentrations. Thus when force-constant changes are important, it is not worthwhile attempting to find solutions to (2.8), with **C** in its present form, to better than first order in the concentration c. There are no difficulties of this nature when only mass changes are considered.

It is convenient to adopt a slightly different notation at this point. The defect atoms are labeled i, are at the sites l_i, and produce changes at the small set of sites s_i around l_i because of the force-constant changes. Then (2.8) becomes

$$\mathbf{G}(l,l';\omega)=\mathbf{P}(l,l';\omega)+\sum_i\sum_{s_i}\sum_{s_i'}\mathbf{P}(l,s_i;\omega)\mathbf{C}^{\delta(l_i)}(s_i,s_i';\omega)\times\mathbf{G}(s_i',l';\omega).\quad(2.10)$$

It is reasonable to assume that $\mathbf{G}(l,l';\omega)$ is dominated by whether or not the sites l or l' are affected by an individual defect matrix. This suggests separating out the Green's functions associated with a given defect as follows:

$$\sum_{s_i'}\left[\mathbf{I}\delta(s_i,s_i')-\sum_{s_i''}\mathbf{P}(s_i,s_i'';\omega)\mathbf{C}^{\delta(l_i)}(s_i'',s_i';\omega)\right]\times\mathbf{G}(s_i',l';\omega)=\sum_{s_i'}\mathbf{X}^{\delta(l_i)}(s_i,s_i';\omega)\mathbf{G}(s_i',l';\omega)=\mathbf{G}^{\delta(l_i)}(s_i,l';\omega),\quad(2.11)$$

where

$$\mathbf{G}^{\delta(l_i)}(l,l';\omega)=\mathbf{P}(l,l';\omega)+\sum_{j\neq i}\sum_{s_js_j'}\mathbf{P}(l,s_j;\omega)\times\mathbf{C}^{\delta(l_j)}(s_j,s_j';\omega)\mathbf{G}(s_j',l';\omega).\quad(2.12)$$

Then (2.10) becomes, on inverting (2.11),

$$\mathbf{G}(l,l';\omega)=\mathbf{P}(l,l';\omega)+\sum_i\sum_{s_is_i'}\mathbf{P}(l,s_i;\omega)\times\mathbf{T}^{\delta(l_i)}(s_i,s_i';\omega)\mathbf{G}^{\delta(l_i)}(s_i',l';\omega),\quad(2.13)$$

and $\mathbf{G}^\delta$ is given by

$$\mathbf{G}^{\delta(l_i)}(l,l';\omega)=\mathbf{P}(l,l';\omega)+\sum_{j\neq i}\sum_{s_js_j'}\mathbf{P}(l,s_j;\omega)\times\mathbf{T}^{\delta(l_j)}(s_j,s_j';\omega)\mathbf{G}^{\delta(l_j)}(s_j',l';\omega).\quad(2.14)$$

T is the usual t matrix describing the scattering of lattice excitations due to the perturbation introduced by one defect atom in an otherwise pure crystal.[17] It is given by

$$\mathbf{T}^{\delta(l_i)}(s_i,s_i';\omega)=\sum_{s_i''}\mathbf{C}^{\delta(l_i)}(s_i,s_i'';\omega)\times\mathbf{X}^{\delta(l_i)}(s_i'',s_i';\omega)^{-1}.\quad(2.15)$$

Equations (2.13) and (2.14) are now averaged over all configurations of defects. We no longer need to use the special symbols for the perturbed sites. The average of the summation on the right-hand side of (2.13) can be written in terms of a conditionally averaged $\mathbf{G}^\delta$,

$$\sum_{l_1l_2}\sum_{l_i}\mathbf{P}(l,l_1;\omega)\langle\mathbf{T}^{\delta(l_i)}(l_1,l_2;\omega)\mathbf{G}^{\delta(l_i)}(l_2,l';\omega)\rangle=\sum_{l_1l_2l_3}\mathbf{P}(l,l_1;\omega)\sum_\delta c^\delta\mathbf{T}^{\delta(l_3)}(l_1l_2;\omega)\times\langle\mathbf{G}^{\delta(l_3)}(l_2,l';\omega)\rangle_{\delta(l_3)}.\quad(2.16)$$

$\langle\ \rangle$ denotes an average over all configurations and $\langle\ \rangle_{\delta(l_i)\delta(l_j)\ldots}$ an average conditional on a defect of type $\delta(l_i)$ at l_i, etc. The probability that a defect is at l_i is given by the concentration of such defects, c^δ. The equation for $\mathbf{G}^\delta$ can be treated in an identical manner. The final equations for $\langle\mathbf{G}\rangle$ and $\langle\mathbf{G}^\delta\rangle_\delta$ are

$$\langle\mathbf{G}(l,l';\omega)\rangle=\mathbf{P}(l,l';\omega)+\sum_{l_1l_2l_3}\mathbf{P}(l,l_1;\omega)\times\sum_\delta c^\delta\mathbf{T}^{\delta(l_3)}(l_1,l_2;\omega)\langle\mathbf{G}^{\delta(l_3)}(l_2,l';\omega)\rangle_{\delta(l_3)}\quad(2.17)$$

and

$$\langle\mathbf{G}^{\delta(l_3)}(l,l';\omega)\rangle_{\delta(l_3)}=\mathbf{P}(l,l';\omega)+\sum_{l_1l_2}\sum_{l_4\neq l_3}\mathbf{P}(l,l_1;\omega)\times\sum_\delta c^\delta\mathbf{T}^{\delta(l_4)}(l_1,l_2;\omega)\langle\mathbf{G}^{\delta(l_4)}(l_2,l';\omega)\rangle_{\delta(l_3)\delta(l_4)}.\quad(2.18)$$

Except where explicitly indicated, the sums on the lattice site labels are now over all sites. It is seen that a $\mathbf{G}^\delta$ conditionally averaged on r sites is always given in terms of $\mathbf{G}^\delta$'s conditionally averaged on $r+1$ sites, thus generating an infinite set of equations which can only be terminated by making an approximation.

The special Green's function $\mathbf{G}^{\delta(l_1)}(l,l';\omega)$ can be interpreted as the effective field, as seen by the atoms at the sites involved in the perturbation, caused by a defect at l_1, due to a disturbance originating at l'. The wave has been allowed to scatter off all the other defects in the crystal before it scatters off the perturbation due to the defect at l_1. The t matrix describes this "final" scattering explicitly in (2.17). The effective-field Green's function will depend, in general, upon the type of defect it refers to as well as the configuration of the other defects in the crystal. We expect it to be made up of a mean part depending only upon the defect type and a random part that depends mainly upon the local environment. It is necessary to proceed to at least the conditional average on two sites to include this random part.

The simplest approximation is to neglect the effect of variations in the local environment and hence the

---

[17] M. V. Klein, Phys. Rev. **131**, 1500 (1963).

random part of the effective-field Green's function, i.e., put

$$\langle \mathbf{G}^{\delta(l_2)}(l,l';\omega)\rangle_{\delta(l_2)\delta(l_3)} \approx \langle \mathbf{G}^{\delta(l_2)}(l,l';\omega)\rangle_{\delta(l_2)}. \quad (2.19)$$

This has the somewhat unfortunate consequence of making $\langle \mathbf{G}^{\delta}\rangle_{\delta}$ independent of δ, as the remainder of the crystal has been replaced by some kind of homogeneous crystal. In particular, this approximation will be valid at small concentrations when there is only a small probability for adjacent defects. This point will be discussed further in the next section.

We then find

$$\sum_{l_1} [\mathbf{I}\delta(l,l_1) - \mathbf{P}(l,l_2;\omega)\sum_{\delta} c^{\delta}\mathbf{T}^{\delta(l_3)}(l_2,l_1;\omega)] \times \langle \mathbf{G}^{\delta(l_3)}(l_1,l';\omega)\rangle_{\delta(l_3)} = \sum_{l_1} \mathbf{Y}(l,l_1;\omega) \times \langle \mathbf{G}^{\delta(l_3)}(l_1,l';\omega)\rangle_{\delta(l_3)} = \langle \mathbf{G}(l,l';\omega)\rangle. \quad (2.20)$$

Finally

$$\langle \mathbf{G}(l,l';\omega)\rangle = \mathbf{P}(l,l';\omega) + \sum_{l_1l_2l_3l_4} \mathbf{P}(l,l_1;\omega) \times \sum_{\delta} c^{\delta}\mathbf{T}^{\delta(l_3)}(l_1,l_2;\omega)\mathbf{Y}^{-1}(l_2,l_4;\omega)\langle \mathbf{G}(l_4,l';\omega)\rangle. \quad (2.21)$$

When only one type of mass defect is present in a cubic system, (2.21) has a much simpler form

$$\langle \mathbf{G}_{\alpha\beta}(l,l';\omega)\rangle = \mathbf{P}_{\alpha\beta}(l,l';\omega) + \sum_{\gamma l_1} P_{\alpha\gamma}(l,l_1;\omega) \times \frac{M_{\gamma}c\epsilon_{\gamma}\omega^2}{1-(1-c)M_{\gamma}\epsilon_{\gamma}\omega^2 P_{\gamma\gamma}(0,0;\omega)} \langle G_{\gamma\beta}(l_1,l';\omega)\rangle. \quad (2.22)$$

We previously obtained this result[4] by both an iterative method and an intuitive approach which was a much simplified form of the above argument. The application of (2.22) to calculating the density of states, optical absorption coefficient, and neutron scattering cross sections for an imperfect crystal with a small concentration of mass defects is discussed at length in that reference. If the factor $\mathbf{Y}^{-1}$ in (2.21) is neglected, and thus the factor $(1-c)$ in (2.22) which arises from it, the result is equivalent to those of Langer,[2] Maradudin,[3] and Takeno.[18] The $(1-c)$ factor has the important effect for a light defect $(0<\epsilon<1)$ of putting the impurity band astride the local-mode frequency due to one mass defect in the crystal. In the earlier work[2,3,18] the bottom of the impurity band lay slightly higher than this frequency.

Although the result for small concentrations is not new, the calculation has been presented in some detail as it gives a different viewpoint on the approximations leading to (2.21). All the previous methods are based on an iterative procedure. Further, it suggests lines of possible improvement that may be possible to evaluate numerically such as including the effects of nearest-neighbor defects or allowing for the random part of the effective-field Green's function in some simple manner. Such possibilities are presently being investigated.

The general approach described in this section was given originally by Lax[10] to describe multiple scattering in a medium of randomly distributed isotropic scatterers with the emphasis upon obtaining the refractive index of the medium.

3. SELF-CONSISTENT CALCULATION FOR FINITE CONCENTRATIONS

Following the discussion after (2.9), we confine our attention to mass defects in describing a method suitable for large c. On iterating (2.8), it is clear that the general form of the result is

$$\langle \mathbf{G}(l,l';\omega)\rangle = \mathbf{P}(l,l';\omega) + \sum_{l_1l_2} \mathbf{P}(l,l_1;\omega) \times \mathbf{\Sigma}(l_1,l_2;\omega)\langle \mathbf{G}(l_2,l';\omega)\rangle. \quad (3.1)$$

The summations are over all lattice sites. In (2.21) and (2.22) we have given a small-c approximation for $\mathbf{\Sigma}$. We introduce a new self-energy $\mathbf{E}$ which will eventually be our approximation for $\mathbf{\Sigma}$. A new Green's function $\mathbf{G}^0$ is defined in terms of $\mathbf{E}$,

$$\mathbf{G}^0(l,l';\omega) = \mathbf{P}(l,l';\omega) + \sum_{l_1l_2} \mathbf{P}(l,l_1;\omega)\mathbf{E}(l_1,l_2;\omega) \times \mathbf{G}^0(l_2,l';\omega). \quad (3.2)$$

Then writing (2.8) in terms of $\mathbf{G}^0$ rather than $\mathbf{P}$, we obtain

$$\mathbf{G}(l,l';\omega) = \mathbf{G}^0(l,l';\omega) + \sum_{l_1l_2} \mathbf{G}^0(l,l_1;\omega) \times \mathbf{V}^{\delta(l_2)}(l_1,l_2;\omega)\mathbf{G}(l_2,l';\omega), \quad (3.3)$$

with

$$\mathbf{V}^{\delta(l_2)}(l_1,l_2;\omega) = -\mathbf{E}(l_1,l_2;\omega) \text{ for a host atom at } l_2\ (\delta=h) \quad (3.4a)$$

$$= -\mathbf{E}(l_1,l_2;\omega) + M\epsilon\omega^2\delta(l_1,l_2)\mathbf{I} \text{ for a defect atom at } l_2(\delta=d). \quad (3.4b)$$

Equation (3.3) has the same form as (2.8), so we can immediately proceed to the equivalent of (2.17),

$$\langle \mathbf{G}(l,l';\omega)\rangle = \mathbf{G}^0(l,l';\omega) + \sum_{l_1l_2} \mathbf{G}^0(l,l_1;\omega)\sum_{\delta} c^{\delta} \times \mathbf{T}^{\delta(l_2)}(l_1,l_2;\omega)\langle \mathbf{G}^{\delta(l_2)}(l_2,l';\omega)\rangle_{\delta(l_2)}. \quad (3.5)$$

Note that $\mathbf{T}$ is now calculated in terms of $\mathbf{G}^0$ rather than $\mathbf{P}$.

If we now identify $\mathbf{E}$ with the exact $\mathbf{\Sigma}$, then $\mathbf{G}^0$ becomes equal to the exact $\langle \mathbf{G}\rangle$ and the scattering term on the right-hand side of (3.5) is equal to zero. However, as we have seen in Sec. 2, (3.5) is just the first equation of an infinite set and approximations are necessary. The principle of our method is to set the scattering

---

[18] S. Takeno, Progr. Theoret. Phys. (Kyoto) **28**, 33 (1962); Suppl. **23**, 94 (1962).

term equal to zero after making the approximation necessary to terminate the set of equations. This will then give a "best" value for $\mathbf{E}$ as our approximation to $\mathbf{\Sigma}$.

The simplest approximation, and the one we will adopt, is to again neglect the random part of the effective-field Green's function and use (2.19). That we are using the same form of approximation for both small and large c may seem strange, but the difference lies in the use of $\mathbf{G}^0$ rather than $\mathbf{P}$ in calculating the t matrices in the present case.

Whether or not other defects are present near a given defect can have a considerable effect on the vibrational frequencies of the defect. However, for small c there is only a small probability for such configurations, and the local environment tends to be that of the perfect crystal. Thus for small c we calculate the t matrix using $\mathbf{P}$ and neglect the effects of environmental fluctuations because, although they can be large, they occur with small probability.

At large c, a given defect has in general a considerable number of other defects in its local environment which tends to look like the imperfect crystal. This justifies the use of the modified Green's function to calculate the t matrices in the present case. Hence we neglect the fluctuations at large c, because, although they are large in number, they are mainly weak in strength.

In one dimension, this is a poor approximation, as the local environment constitutes a small number of sites as compared with three dimensions. In fact, Dean[7] has shown that the considerable structure found in his machine calculations even at low concentrations of light defects is due to the local environment. Even in three dimensions, at a given low defect concentration, the approximation should be better for heavy defects. We can expect that the modes in the impurity band are still fairly well localized, even at finite defect concentrations, whereas the heavy-defect resonant modes are never localized. Hence the local environment effects should be most important in the impurity band.

In the present situation, all the functions in (2.21) depend only upon the distance between the two sites indicated so we can Fourier transform to $\mathbf{k}$ space. Our condition for obtaining $\mathbf{E}$ then gives

$$\sum_{\delta} c^{\delta}\mathbf{T}^{\delta}(\mathbf{k},\omega)=0. \qquad (3.6)$$

The simplest possible approximation for large concentrations of defects is the virtual crystal where $\mathbf{E}(\omega)=Mc\epsilon\omega^2\mathbf{I}$, obtained by replacing $\mathbf{T}^{\delta}$ by $\mathbf{V}^{\delta}$ in (3.6). To obtain the correct description of the local or resonant modes due to one defect, it is necessary to proceed beyond the first iteration of (2.8) to obtain the t matrix. Intuitively, (3.6) is thus seen to be a reasonable first approximation for large c. Any better approximation will weight the t matrices $\mathbf{T}^h$ and $\mathbf{T}^d$ differently by the different effective fields $\mathbf{G}^h$ and $\mathbf{G}^d$.

Using the explicit forms of $\mathbf{V}$, (3.4), with $c^d=c$ and $c^h=1-c$, we find

$$\mathbf{E}(\mathbf{k},\omega)\left[\mathbf{I}+\frac{1}{N}\sum_{\mathbf{k}}\mathbf{G}^0(\mathbf{k},\omega)\mathbf{E}(\mathbf{k},\omega)\right]^{-1} \times\left[\mathbf{I}-(1-c)M\epsilon\omega^2\mathbf{G}^0(\omega)+\frac{1}{N}\sum_{\mathbf{k}}\mathbf{G}^0(\mathbf{k},\omega)\mathbf{E}(\mathbf{k},\omega)\right] =Mc\epsilon\omega^2\mathbf{I}, \qquad (3.7)$$

where

$$\mathbf{G}^0(\omega)=\mathbf{G}^0(l,l;\omega)=\frac{1}{N}\sum_{\mathbf{k}}\mathbf{G}^0(\mathbf{k},\omega). \qquad (3.8)$$

Thus $E(\mathbf{k},\omega)$ is independent of $\mathbf{k}$, and further simplification gives

$$\mathbf{E}(\omega)-Mc\epsilon\omega^2\mathbf{I}-\mathbf{E}(\omega)[M\epsilon\omega^2\mathbf{I}-\mathbf{E}(\omega)]\mathbf{G}^0(\omega)=0. \qquad (3.9)$$

$\mathbf{G}^0$ is also related to $\mathbf{E}$ by (3.2) in terms of $\mathbf{P}$ which is given by (I)

$$P_{\alpha\beta}(l,l';\omega)=\frac{1}{N(M_\alpha M_\beta)^{1/2}} \times\sum_{j\mathbf{k}}\frac{\sigma_\alpha{}^{j*}(\mathbf{k})\sigma_\beta{}^{j}(\mathbf{k})e^{-i\mathbf{k}\cdot(\mathbf{R}_l-\mathbf{R}_{l'})}}{\omega^2-\omega_j{}^2(\mathbf{k})}. \qquad (3.10)$$

$\sigma_\alpha{}^j(\mathbf{k})$ and $\omega_j(\mathbf{k})$ are the eigenvector and eigenfrequency for the $(j,\mathbf{k})$ normal mode of the perfect crystal. In particular, in a monatomic cubic crystal

$$P_{\alpha\beta}(l,l;\omega)=\delta_{\alpha\beta}P(\omega). \qquad (3.11)$$

It is then consistent to assume $\mathbf{E}(\omega)$ is diagonal and rewrite (3.9) in the form

$$\tilde{\epsilon}(\omega)-c\epsilon=\tilde{\epsilon}(\omega)[\epsilon-\tilde{\epsilon}(\omega)]\omega^2G^0(\omega), \qquad (3.12)$$

with

$$\mathbf{E}(\omega)=M\tilde{\epsilon}(\omega)\omega^2\mathbf{I} \qquad (3.13)$$

and

$$G^0(\omega)=\int\frac{\nu(\omega')d\omega'}{\omega^2[1-\tilde{\epsilon}(\omega)]-\omega'^2}. \qquad (3.14)$$

Equation (3.14) is obtained from (3.2), (3.10), and (3.13), on replacing the summation over the quasi-continuous set of modes $(j,\mathbf{k})$ by an integration over ω' and using a phonon density of states for the perfect crystal $\nu(\omega')$ that is normalized to unity.

As G^0 and $\tilde{\epsilon}$ must have the same analytic behavior, then, in regions of zero density of states where $\mathrm{Im}\,\tilde{\epsilon}(\omega)=0$,

$$\tilde{\epsilon}(\omega)\leq\frac{\omega^2-\omega_m{}^2}{\omega^2} \qquad (3.15)$$

or

$$\tilde{\epsilon}(\omega)\geq 1,$$

where ω_m is the maximum frequency in the phonon density of states $\nu(\omega)$. There is no requirement that $\tilde{\epsilon}(\omega)$ should diverge in any gap that might develop in the density of states although we shall see in Sec. 5 that for certain values of ϵ and c it can do so.

Upon the solution of the self-consistent equation (3.12) we can obtain several correlation functions that describe some of the dynamical properties of the imperfect crystal. The density of states is given by

$$\nu'(\omega)=\frac{2}{\pi\omega}\int \nu(\omega')d\omega'\,\mathrm{Im}\frac{\omega'^2}{\omega^2[1-\tilde{\epsilon}(\omega)]-\omega'^2}. \qquad (3.16)$$

In the one-phonon approximation, the neutron scattering cross section[19] is given by (I)

$$\frac{d^2\sigma}{d\Omega dE}=\frac{k_2}{\pi M k_1}\frac{e^{\beta\omega}}{e^{\beta\omega}-1}\times[S_{\mathrm{coh}}'(\mathbf{k},\omega)+S_{\mathrm{incoh}}'(\mathbf{k},\omega)], \qquad (3.17)$$

$$S_{\mathrm{coh}}'(\mathbf{k},\omega)=\langle A\rangle_{\mathrm{av}}^2\sum_j[\mathbf{k}\cdot\boldsymbol{\sigma}^j(\mathbf{k})]^2\,\mathrm{Im}G_j^0(\mathbf{k},\omega), \qquad (3.18)$$

$$S_{\mathrm{incoh}}'(\mathbf{k},\omega)=(\langle A^2\rangle_{\mathrm{av}}-\langle A\rangle_{\mathrm{av}}^2)k^2\,\mathrm{Im}G^0(\omega), \qquad (3.19)$$

for a neutron scattered from $\mathbf{k}_1$ to $\mathbf{k}_2$, $\mathbf{k}=\mathbf{k}_1-\mathbf{k}_2$, into solid angle $d\Omega$ with energy change $E=\hbar\omega$. $\langle A^2\rangle_{\mathrm{av}}$ and $\langle A\rangle_{\mathrm{av}}$ are the thermal averages over the scattering lengths of the spin states of the scattering nucleus and include the Debye-Waller factor. We have assumed equal scattering lengths for both defect and host atoms, but this restriction can be lifted by using methods described in I. The result is to produce the following replacements in (3.18) and (3.19):

$$\begin{aligned}\langle A^2\rangle_{\mathrm{av}}&\to\left[1-\frac{\tilde{\epsilon}(\omega)}{\epsilon}\right]\langle A_h^2\rangle_{\mathrm{av}}+\frac{\tilde{\epsilon}(\omega)}{\epsilon}\langle A_d^2\rangle_{\mathrm{av}},\\ \langle A\rangle_{\mathrm{av}}&\to\left[1-\frac{\tilde{\epsilon}(\omega)}{\epsilon}\right]\langle A_h\rangle_{\mathrm{av}}+\frac{\tilde{\epsilon}(\omega)}{\epsilon}\langle A_d\rangle_{\mathrm{av}}.\end{aligned} \qquad (3.20)$$

The behavior, with respect to c and ω, of the three correlation functions in (3.16), (3.18), and (3.19) will be described in Sec. 5 along with the numerical solution of (3.12).

Because of the form of (3.16), the density of states will remain correctly normalized to unity for all c. We have previously shown (I) that the exact $G(\omega)$ must satisfy the following sum rule under all circumstances:

$$\frac{1}{M^h}\int_{-\infty}^{\infty}\omega\,\mathrm{Im}G(\omega)d\omega=\pi\left[\frac{c^h}{M^h}+\frac{c^d}{M^d}\right]. \qquad (3.21)$$

It is easy to show that $G^0(\omega)$, in our approximation, still satisfies this sum rule.

4. OTHER SELF-CONSISTENT CALCULATIONS

Davies and Langer[6] have given the only other self-consistent calculation for the dynamics of an imperfect crystal. In the small-concentration result (2.22), we see that the self-energy is real for $\omega>\omega_m$ as $P(\omega)$ is real in this region. However, for suitable $\epsilon(0<\epsilon<1)$, an impurity band can form in this region. Thus G is complex, but the self-energy is real in the impurity band. Davies and Langer removed this inconsistency by replacing the unperturbed Green's function by the perturbed function in the t matrix in Langer's first-order result.[2] Their resulting self-consistent equation for the one-dimensional case is

$$\gamma(\omega)=c\lambda\left[1-\frac{\lambda}{N}\sum_k\frac{\omega_k^2}{\omega^2-\omega_k^2[1+\gamma(\omega)]}\right]^{-1}, \qquad (4.1)$$

with

$$\lambda=\epsilon/(1-\epsilon)$$

and

$$1+\gamma(\omega)\equiv[1-\tilde{\epsilon}(\omega)]^{-1}.$$

Although only introduced from the analytic standpoint, (4.1) could be considered to describe an imperfect crystal with a value of c that is greater than that for which the first-order theory is valid. The reasoning is similar to that used in giving meaning to the use of G^0 to calculate the t matrices in Sec. 3. Equation (4.1) leads to a quartic equation for a function whose imaginary part is the density of states for the imperfect crystal. On solving this equation with $\epsilon=\frac{2}{3}$, we find that the top of the impurity band has exceeded the frequency $\omega_m'=\omega_m(1-\epsilon)^{-1/2}$ by $c=0.15$, although the gap between the main band and the impurity band does not close till around $c=0.22$. This is a highly unphysical result for there can be no frequencies in the system which exceed the maximum frequency of a crystal made entirely of the light-defect atoms, as follows from the arguments of Rayleigh.[20]

This result is undoubtedly due to the fact that the defect and host atoms have not been considered on an equivalent basis. For a disordered crystal containing atoms of mass M^A and M^B, the final result for the correlation functions and the density of states should be independent of which type of atom is considered as host. If $(\boldsymbol{\epsilon}^A,\boldsymbol{\Sigma}^A(\mathbf{k},\omega))$ describes such a crystal with the type-A atoms considered as host and $(\boldsymbol{\epsilon}^B,\boldsymbol{\Sigma}^B(\mathbf{k},\omega))$ describes the opposite situation, then this defect-host symmetry applied to (3.1) leads to the relation

$$M^A\epsilon^A\boldsymbol{\Sigma}^B(\mathbf{k},\omega)+M^B\epsilon^B\boldsymbol{\Sigma}^A(\mathbf{k},\omega)=M^AM^B\epsilon^A\epsilon^B\omega^2\mathbf{I}. \qquad (4.2)$$

Our result, (3.12), satisfies (4.2), whereas (4.1) does not. It would seem necessary that any theory describing large defect concentrations should satisfy this symmetry condition.

Recently Yonezawa and Matsubara[21] have shown what is necessary to give the iterative type of solution this symmetry. On averaging the iterated form of

---

[19] L. Van Hove, Phys. Rev. **95**, 249 (1954).

[20] See for instance A. A. Maradudin, E. W. Montroll, and G. H. Weiss, Solid State Phys. Suppl. No. 3 (1963).

[21] F. Yonezawa and T. Matsubara, Progr. Theoret. Phys. (Kyoto) **35**, 357 (1966).

(2.8), care has to be taken that no more than one defect can be on a given site. This necessitates partitioning all lattice-site summations such that none of the summation indices can be the same. After averaging, these restrictions must be removed in some manner to enable a closed form of the solution to be obtained. Langer's first-order result for the self-energy is obtained by summing only those proper diagrams containing one defect vertex and treating the restricted summations by a random-phase approximation.[18] However, if the restricted summations are treated exactly, these first-order proper diagrams are multiplied by a set of polynomials in c rather than just c. Leath and Goodman[22] have recently evaluated these polynomials. Parts of these polynomials arise from treating the restricted summations which contain factors equivalent to proper diagrams with more than one defect vertex. In I we obtained the $(1-c)$ factor in (2.22) by neglecting these contributions to the polynomials in evaluating the restricted summations. Yonezawa and Matsubara give a calculation similar to that of Leath and Goodman but for the equivalent electron problem. They further demonstrate that if the result is made self-consistent by the same method used by Davies and Langer, it then satisfies the defect-host symmetry condition. The resulting self-consistent equation is, in our language,

$$\bar{\epsilon}(\omega)=\int_0^\infty dt\, e^{-t}\frac{c\epsilon\exp[t\epsilon\omega^2G^0(\omega)]}{1-c+c\exp[t\epsilon\omega^2G^0(\omega)]}. \tag{4.3}$$

This is more complicated to solve than our result (3.12) and does not appear to satisfy the sum rule (3.21).

We note that Maris[23] has recently given a treatment for a disordered crystal that is valid at all concentrations. It involves an expansion in $\epsilon/(1-\epsilon)$ which is only taken to third order, self-consistency being included to prevent divergences. As such it is only applicable to small changes in mass and cannot describe the behavior of the impurity bands that arise from the local modes.

5. SOLUTION OF THE SELF-CONSISTENT EQUATION

A. One Dimension

As we discussed in Sec. 3, the approximation (2.19) leading to (3.12) is rather poor in one dimension at finite concentrations. Thus we give only a brief description of the one-dimensional solution of (3.12), mainly to afford a comparison with the previous self-consistent calculation of Davies and Langer.[6]

For a linear chain, connected by nearest-neighbor spring-force constants, $G^0(\omega)$ is easily evaluated[2]:

$$G^0(\omega+i0^+)=\frac{-i}{\omega_m{}^2x[1-\bar{\epsilon}(x)]^{1/2}\{1-x^2[1-\bar{\epsilon}(x)]\}^{1/2}}, \tag{5.1}$$

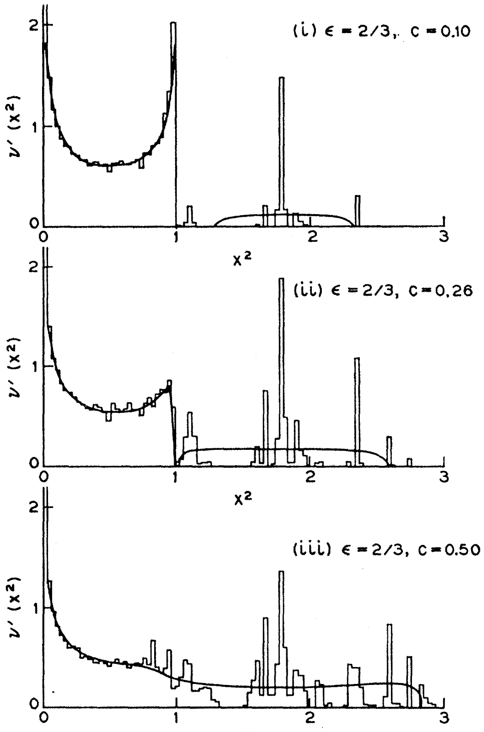

FIG. 1. Comparison in one dimension between the self-consistent calculation (solid line) and Dean's calculations (histogram) for $\epsilon=\frac{2}{3}$ and (i) $c=0.10$, (ii) $c=0.26$, (iii) $c=0.50$.

and (3.12) gives a cubic for $\bar{\epsilon}(\omega)$,

$$\begin{aligned} &a_0\bar{\epsilon}(x)^3+a_1\bar{\epsilon}(x)^2+a_2\bar{\epsilon}(x)+a_3=0\,, \qquad (5.2)\\ &a_0=2x^2[1-\epsilon(1-c)]-1\,,\\ &a_1=x^2[\epsilon^2(1-c^2)-(1+4c\epsilon)]\,,\\ &a_2=c\epsilon[c\epsilon-2(1+c\epsilon)(1-x^2)]\,,\\ &a_3=(c\epsilon)^2(1-x^2)\,. \end{aligned}$$

We consistently use the notation $x=\omega/\omega_m$ throughout the numerical work of this paper.

The density of states is finite when (5.2) has a complex root; the real root that is always present is discarded as unphysical. The density of states, as a function of x^2, is then evaluated using (3.16) for $\epsilon=\frac{2}{3}$ and $c=0.16$, 0.26, 0.50 and compared with Dean's results[7] in Fig. 1. Although none of the structure in the impurity-band region is given by our method, we do seem to have a fair over-all description of the effects of increasing the concentration.

To be able to obtain any of the impurity-band structure, a better approximation than (2.19) is required that takes into account the local environment. Any such procedure will undoubtedly lead to a k-dependent self-energy $E(k,\omega)$, with the resulting integral equation being far more difficult to solve than (3.12).

In Fig. 2 we compare our calculation with that of Davies and Langer for $\epsilon=\frac{2}{3}$ and $c=0.10$. The much broader impurity band of Davies and Langer that

---

[22] P. L. Leath and B. Goodman, Phys. Rev. 148, 968 (1966).
[23] H. J. Maris, Phil. Mag. 13, 465 (1966).

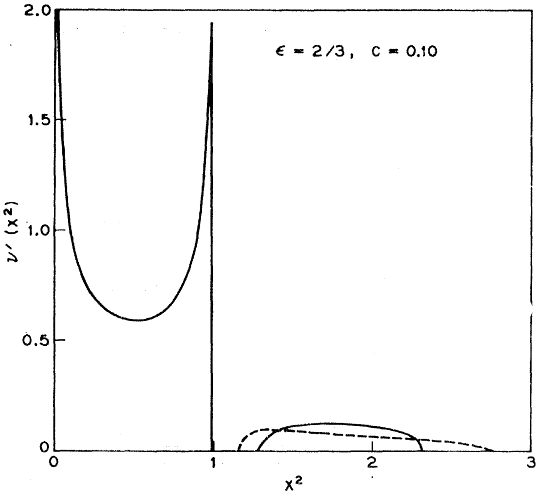

FIG. 2. Comparison in one dimension between our self-consistent calculation (solid line) and that of Davies and Langer (dashed line) for $\epsilon=\frac{2}{3}$, $c=0.10$.

eventually leads to the unphysical condition described in Sec. 4 is clearly seen.

One feature in common between both these self-consistent calculations is the reduction in the maximum frequency of the original phonon band as light defects are added. In this one-dimensional calculation, the change is too small (at most about 2%) to see in Dean's work. However, as we will see in the next part of this section, it is quite appreciable in three dimensions.

B. Three Dimensions

The only information we need about the perfect crystal into which we are introducing the defects is its density of states. As a realistic situation we chose to use the copper density of states due to Sinha.[24] We concentrated upon the case of $\epsilon=-2.1$ as this corresponds to gold in copper, the system investigated by Svensson *et al.*[25] using inelastic neutron scattering.

This density of states is taken as a 42-point histogram, and the integral (3.14) is done analytically in each interval. Equation (3.12) was finally solved by an iterative procedure based on Newton's method applied to a function of a complex variable. A convenient starting point is at low frequencies when we can expect $\mathrm{Re}\,\tilde{\epsilon}(\omega)\approx c\epsilon$ and just give a sufficiently large value for $\mathrm{Im}\,\tilde{\epsilon}(\omega)$ so that the method can converge on a complex root rather than a real one. We then proceed to higher frequencies in small steps of ω, using the previous value of $\tilde{\epsilon}(\omega)$ as a starting point at each stage. Such a procedure works well over most of the frequency range, converging at better than one decimal place per iteration.

However, when a gap develops $\tilde{\epsilon}(\omega)$ varies rapidly with ω in the region around the gap and may even diverge. As a result this proves to be a difficult region to solve (3.12). By choosing a very small frequency interval between successive stages, the solution of (3.12) can always be followed into the gap from below but not from above. This difficulty can be alleviated to some degree when $\tilde{\epsilon}(\omega)$ is large by considering (3.12) as a function of $\tilde{\epsilon}(\omega)^{-1}$.

The various types of behavior of $\tilde{\epsilon}(\omega)$ for $\epsilon=-2.1$ are illustrated in Fig. 3. At $c=0.25$ we see the typical resonant behavior, familiar from the small-concentration results (I), which can be thought of as indicating the frequency at which the heavy defects prefer to oscillate. As the concentration increases this resonant characteristic becomes more exaggerated and moves to higher frequencies. When a gap appears, $\mathrm{Re}\,\tilde{\epsilon}(\omega)$ may diverge as illustrated in Fig. 3(ii) for $c=0.75$. At even larger values of c, $\mathrm{Re}\,\tilde{\epsilon}(\omega)$ takes on a different behavior in the gap with the divergence disappearing as shown in Fig. 3(iii) for $c=0.95$. Although this is a rather low defect concentration for (3.12) to be applicable, it is shown because this type of behvaior dominates for smaller values of the defect-host mass ratio. As expected, $\mathrm{Re}\,\tilde{\epsilon}(\omega)$ has slope discontinuities at the band edges although they are sometimes too small relative to the general slope of $\mathrm{Re}\,\tilde{\epsilon}(\omega)$ to be seen in Fig. 3. The cusp for $c=0.95$ is an extreme example of such a discontinuity.

In the troublesome region at the bottom of the impurity band $\tilde{\epsilon}(\omega)$ is large and we can expand (3.12) in terms of $\tilde{\epsilon}(\omega)^{-1}$. It is necessary to expand out to $\tilde{\epsilon}(\omega)^{-2}$ as the coefficient of the linear term can vanish for certain interesting values of the parameters. It is this vanishing that leads to the change in behavior of $\mathrm{Re}\,\tilde{\epsilon}(\omega)$ in Figs. 3(ii) and 3(iii). The behavior of $\tilde{\epsilon}(\omega)^{-1}$ is shown in Fig. 4 for $c=0.75$, 0.90, and 0.95. As $\mathrm{Re}\,\tilde{\epsilon}(\omega)$ leaves the main band negative in the iteration method, we can immediately see why this method follows the lower (heavy) line in Fig. 4 leading to the two types of behavior shown in Fig. 3. The expansion of the Green's

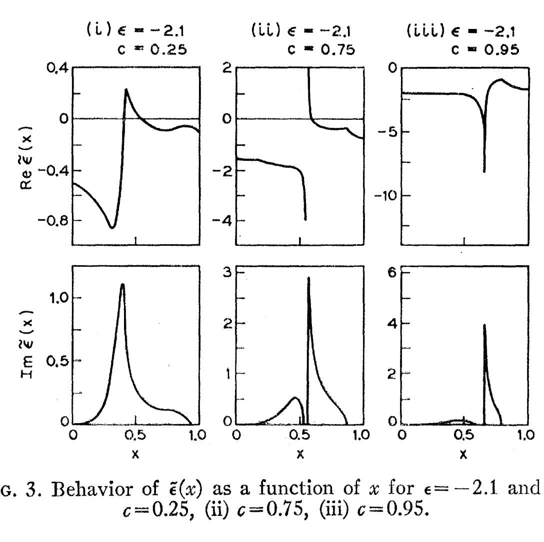

FIG. 3. Behavior of $\tilde{\epsilon}(x)$ as a function of x for $\epsilon=-2.1$ and (i) $c=0.25$, (ii) $c=0.75$, (iii) $c=0.95$.

---

[24] S. K. Sinha, Phys. Rev. 143, 422 (1966).

[25] E. L. Svensson, B. N. Brockhouse, and J. M. Rowe, Solid State Commun. 3, 245 (1965).

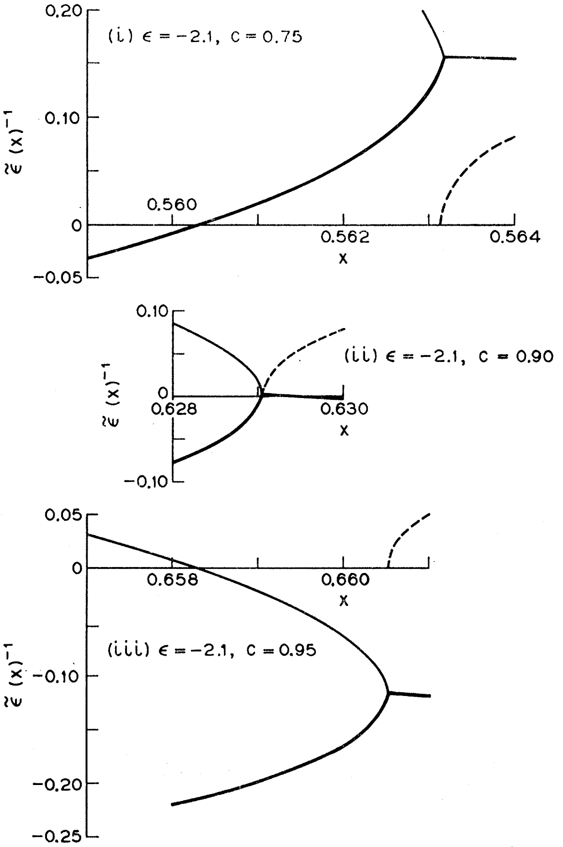

FIG. 4. Behavior of $\tilde{\epsilon}(x)^{-1}$ in the vicinity of the bottom of the impurity band, as given by the expansion of (3.12) in terms of $\tilde{\epsilon}(x)^{-1}$, for $\epsilon=-2.1$ and (i) $c=0.75$, (ii) $c=0.90$, (iii) $c=0.95$. Solid line, $\mathrm{Re}\tilde{\epsilon}(x)^{-1}$; dashed line, $\mathrm{Im}\tilde{\epsilon}(x)^{-1}$. Iteration procedure follows heavy solid line.

function is better the larger the value of ω. The difference between the iteration and expansion values of $\tilde{\epsilon}(\omega)$ around the bottom of the impurity band is less than 5% for $c=0.95$ ($\omega\approx0.66\omega_m$), but of the order of 50% for $c=0.75$ ($\omega\approx0.56\omega_m$).

At the resonance [$\mathrm{Re}\tilde{\epsilon}(\omega)=0$ in Fig. 3(i)] $\mathrm{Im}\tilde{\epsilon}(\omega)$ has the usual peak. As c increases and the gap appears, this peak is split as can be seen in Fig. 3(ii) and 3(iii). The physics of the detailed shape is not clear. However, as we are effectively calculating the response of the crystal to wave-like excitations of definite **k**, it is not surprising that damping of these excitations is much greater in the impurity band, which has formed from the localized modes, as compared with damping of excitations in the main band.

As implied at the beginning of this subsection, if we start out with too small a value of $\mathrm{Im}\tilde{\epsilon}(\omega)$ in the low-frequency region the iteration tends to lock onto a purely real value of $\tilde{\epsilon}(\omega)$. We also note that the expansion procedure indicates the presence of several real roots in the gap. However, we never found any indications of more than one complex root. The real roots can be discarded as unphysical if in the band region [just as we discarded the ever present real root of the cubic (5.2)] or as of no physical interest if in the gap region.

Having evaluated $\tilde{\epsilon}(\omega)$ we are now in a position to obtain the various correlation functions. The behavior of the density of states $\nu'(\omega)$, and $\mathrm{Im}G^0(\omega)$ is shown in Fig. 5. The two functions behave in a similar manner but the different relative magnitudes of their structures could be important experimentally. These numerical results satisfy the sum rule (3.21) and give the correct normalization of $\nu'(\omega)$ to better than 1%, providing a good check on the iteration.

As c increases, the resonant peak grows and widens and eventually begins to show the structure of the pure density of states $\nu(\omega)$. This is not surprising if we consider the peak as being due mainly to the motions of the heavy-defect atoms. The structure due to $\nu(\omega)$ that appears in the peak moves very little with increasing c in contrast to the structure at the larger values of ω which tends to move to lower values of ω. This can be understood to some extent from the arguments of Rayleigh,[20] the modes in the main band being tied down to a large extent by a large number of neighboring ones whereas those in the impurity band are somewhat freer to move.

In Fig. 6, we show the behavior of the band edges as a function of c. The width of the impurity band behaves like $(1-c)^{1/2}$ to the accuracy of our calculations, and its midpoint decreases with decreasing c. The most interesting feature is the reduction in the maximum frequency of the main band as light defects are added ($1-c$ increasing). The erosion of the strength of the top of the main band in forming the impurity band is expected, but our theory indicates that the erosion is so great as to completely remove the top of the band. In a general discussion of the equivalent electron problem, Lifshitz[16] predicts a behavior of the main band edge that is in agreement with our result.

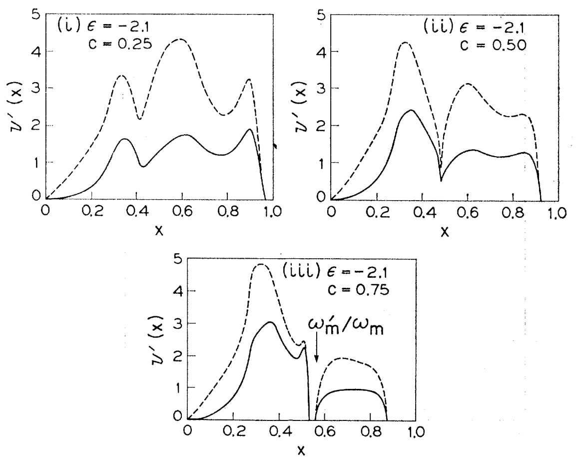

FIG. 5. Density of states $\nu'(x)$ (solid line) and $\mathrm{Im}G^0(x)$ (dashed line) for the imperfect crystal with $\epsilon=-2.1$ and (i) $c=0.25$, (ii) $c=0.50$, (iii) $c=0.75$.

It is of some interest to compare our self-consistent result for the density of states with that given by the small-concentration result (2.22). This is done for $c=0.10$, 0.90 in Fig. 7. The two curves agree quite well for $c=0.10$, which is not too surprising as the fluctuations in the effective field have been neglected in both calculations and there are no analytic inconsistencies in (2.22) in this case. However, it does suggest that the disagreement found by Svensson *et al.*[25] between the frequency shift of the lattice modes, due to 9.3% gold in copper, as given by (2.22) and that obtained from their inelastic coherent neutron scattering data is not a concentration effect. It would thus seem necessary to invoke force-constant changes and/or departures from purely random disorder to explain their result. For $c=0.90$, the two results do not agree in the impurity-band region although the areas under the two curves equal $(1-c)$ (as do all our impurity-band results) and both are centered on the local-mode frequency ω_L. We also note that the small-concentration result gives the width of the impurity band as proportional to $1-c$, in contrast to our result of $(1-c)^{1/2}$. As this is the region where (2.22) has analytic inconsistencies, these differences are to be expected. It can also be argued that these two concentrations are in the no man's land where neither approximation is particularly good.

Some other values of ϵ were briefly investigated to check various trends. For instance, when the ratio of the defect to host mass decreases the gap between the main and impurity bands closes at lower concentrations of the light defect. The trend was not evaluated quantitatively as this is an extremely difficult region in which to solve (3.12). Further, we considered the behavior of $\nu'(\omega)$ when the value of ϵ is less than that required to produce a local mode ($\epsilon_{cr}=0.35$ for the copper density of states in use). As the concentration of the light defects is increased, a shoulder develops on the density of states above ω_m instead of a separate impurity band. There is also a drift of the structure of $\nu'(\omega)$ to higher frequencies with increasing defect concentration. This is to be contrasted to the previously described situation for $\epsilon>\epsilon_{cr}$ but is in general agreement with the discussions of both Takeno[18] and Lifshitz.[16]

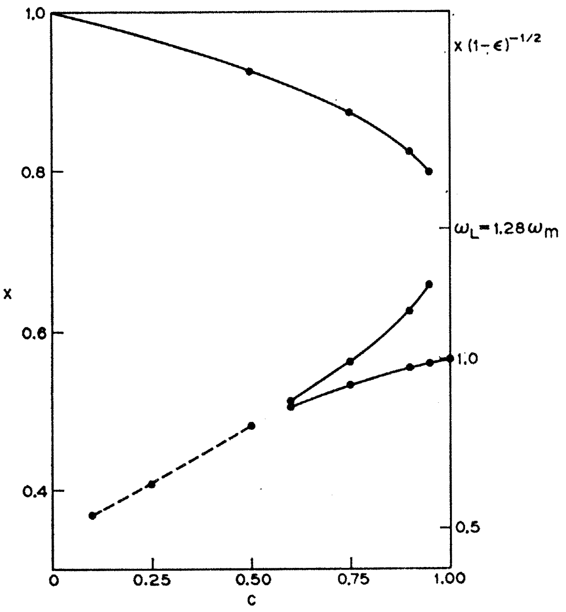

FIG. 6. Behavior of the band edges as a function of c for $\epsilon=-2.1$. The dashed line gives the position of the resonance $[\mathrm{Re}\tilde{\epsilon}(\omega)=0]$. The computed points are indicated by the solid circles.

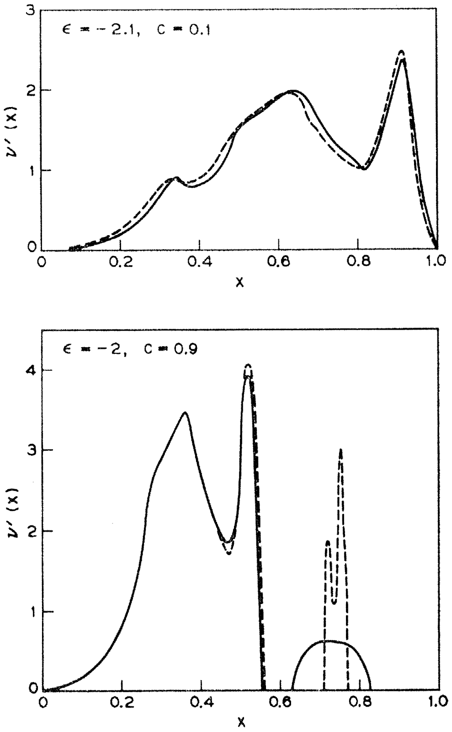

FIG. 7. Comparison between self-consistent (solid line) and first-order (dashed line) densities of states for $\epsilon=-2.1$ and $c=0.10$ and 0.90.

The spectral function is given by

$$\mathrm{Im}G^j(\mathbf{k},\omega)=\frac{\omega^2\,\mathrm{Im}\tilde{\epsilon}(\omega)}{\{\omega^2[1-\mathrm{Re}\tilde{\epsilon}(\omega)]-\omega_j^2(\mathbf{k})\}^2+[\omega^2\,\mathrm{Im}\tilde{\epsilon}(\omega)]^2}. \quad (5.3)$$

The behavior of its peaks as a function of c indicates how the presence of defects shifts the phonon frequencies, such as would be seen by coherent neutron scattering (3.18). This function contains a considerable amount of detailed information about the dynamics of the imperfect crystal and as a consequence suffers most from our approximation.

The spectral function tends to show a response at two frequencies (for c nonzero). For low c, one of these may be identified as being due to the heavy-defect resonance and the other is near $\omega_j(\mathbf{k})$. For $\omega_j(\mathbf{k})$ well away from the resonance, the response at the reso-

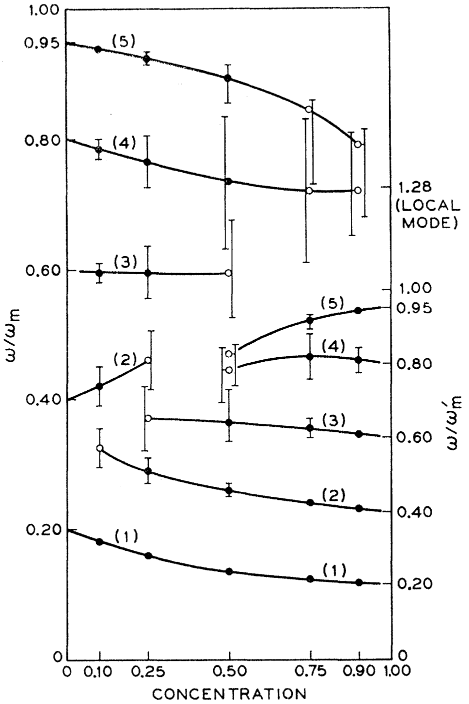

FIG. 8. Concentration dependence of the positions and half-maximum points of the spectral function (5.3) with $\epsilon=-2.1$; (1) $\omega_j(\mathbf{k})=0.2\omega_m$, (2) $\omega_j(\mathbf{k})=0.4\omega_m$, (3) $\omega_j(\mathbf{k})=0.6\omega_m$, (4) $\omega_j(\mathbf{k})=0.8\omega_m$, (5) $\omega_j(\mathbf{k})=0.95\omega_m$. In the case of two peaks the stronger is indicated by the solid circle, the weaker by the open circle.

nance is very weak. Otherwise, the two responses are of comparable magnitude and quite broad. At large defect concentrations ($c\approx 0.5$) this large width may result in the weaker response being merely a shoulder on the larger peak. In Fig. 8 we show the positions of the maxima of these response peaks, when they are definitely resolved, for a representative set of values of $\omega_j(\mathbf{k})$. If the sizes of the maxima do not differ by more than about an order of magnitude, the larger is indicated by a solid circle and the smaller by an open circle. Otherwise only the position of the dominant peak is shown. The error bars indicate the half-maximum points of the peaks which can be quite asymmetric due to the strong frequency dependence of $\bar{\epsilon}(\omega)$. In the impurity-band region it is seen that the response can be very broad, sometimes too broad to be called a peak.

In general, the frequency of a given $(j,\mathbf{k})$ mode does not change smoothly as c increases from zero to unity. As c increases, the peak associated with $\omega_j(\mathbf{k})$ reduces in strength and broadens into an impurity-band peak whereas the rather broad resonant peak increases in strength, becoming narrower, and eventually becomes the $\omega_j(\mathbf{k})$ peak for the pure crystal with $c=1$. Only when $\omega_j(\mathbf{k})$ is less than the resonant frequency does the position of the peak associated with $\omega_j(\mathbf{k})$ change continuously with all values of c. However, when the mass ratio is so small that there can be no local mode, there is only one dominant peak which moves smoothly with concentration in a similar manner to that predicted by the virtual crystal approximation.

6. COMPARISON WITH OTHER WORK ON DISORDERED CRYSTALS

A. Machine Calculations

Payton and Visscher[9] (PV) have recently made an extensive study of disordered crystals using high-speed computers. They use the Sturm sequence method first used by Dean[7] in one dimension and by Dean and Bacon[8] in two dimensions. However, besides studying the effects of force-constant changes and departures from purely random disorder, they have extended the calculations to three dimensions. These results provide an excellent test for the density of states given by our theory.

We use a density of states for a simple cubic crystal that was evaluated by PV using the same technique as for the disordered crystals. Because of the finite sample they must employ, this density of states is very ragged, but it is largely smoothed out in our calculations by the finite size of $\mathrm{Im}\bar{\epsilon}(\omega)$. We have solved (3.12) using this density of states with $\epsilon=-2$ for $c=0.240$, 0.491, 0.760, and 0.866. The resulting densities of states, as a function of $z=x^2$, are shown in Fig. 9 along with the histograms obtained by PV for these cases.

There is seen to be a very good agreement between our theory and PV's results. However, we do not reproduce the spikey structure they find for low concentrations of light defects. As in one dimension, this structure is due to small islands of defects, i.e., a local environment effect, and so is eliminated by our approximation. PV find that this structure disappears when the defect concentration exceeds the critical percolation concentration. This is the concentration when the probability for the formation of an infinite island of defects in an infinite crystal reaches unity, and it equals 0.28

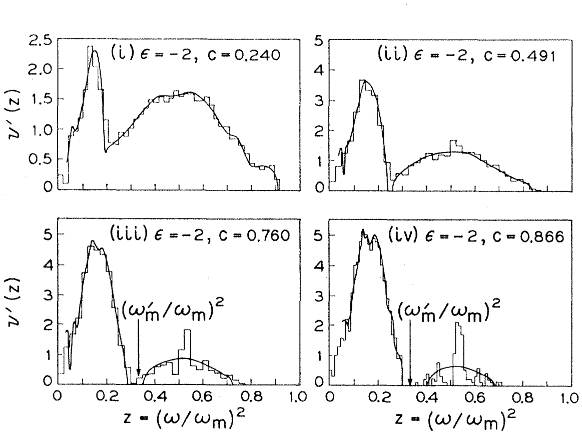

FIG. 9. Comparison of our densities of states (line) with the machine calculations of Payton and Visscher (histogram) for a simple cubic crystal: $\epsilon=-2$, (i) $c=0.240$, (ii) $c=0.491$, (iii) $c=0.760$, (iv) $c=0.866$.

for the simple cubic lattice.[26] For light-defect concentrations greater than this and at low concentrations of heavy defects our results are in excellent agreement with PV's.

A further point is the behavior of the gap between the main and impurity bands. We found in Sec. 5.B that the maximum frequency of the main band decreases as light defects are added. It is seen in Figs. 9(iii) and 9(iv) that this is in agreement with the work of PV. However, our gap persists to larger light-defect concentrations along with the prediction of a slightly narrower impurity band.

The detailed structure at very low frequencies is due to the ragged density of states that we use and to the fact that $\mathrm{Im}\tilde{\epsilon}(\omega)$ goes to zero at zero frequency. Hence we have not pursued the solution of (3.12) into this region.

We would like to thank Dr. Payton for evaluating the histogram densities of states shown in Fig. 9 so that we could make this comparison.

B. Experiments on Disordered Crystals

There are two recent experiments on the dynamical properties of disordered crystals over a range of concentrations. Verleur and Barker[27] have investigated the optical reflectance of the GaAs-P system. This system is too complicated for our theory to apply and they also find there are large departures from purely random disorder. However, it is of interest to note that they find a qualitatively similar behavior of the optically active modes to that which we show in Fig. 8. The frequency of the local mode due to P in GaAs increases smoothly as P is added, eventually approaching the transverse optic (TO) mode for GaP with a similar behavior for the TO mode of GaAs. At large defect concentrations, they see several other modes that they attribute to departures from random disorder.

The Ge-Si system investigated by Logan, Rowell, and Trumbore[11] (LRT) using phonon-assisted electron tunneling in *p-n* junctions is a better case for applying our theory. Although the lattice has two sites per unit cell they are equivalent and the only difficulty is the assumption of just a mass change. An examination of the dispersion curves for Ge [28] and Si [29], as obtained from inelastic neutron scattering experiments, indicates that there are topological differences between the two sets of curves, particularly along Δ, that cannot be obtained by scaling. However, the zone-boundary phonons do scale by between 0.55 and 0.60 $[(M_{\mathrm{Si}}/M_{\mathrm{Ge}})^{1/2}=0.62]$ and, as the experiments see phonons out towards the zone boundary, it seems worth while to pursue the comparison.

The mimimum conduction-band energy in Ge is at L and along Δ at about (0.85, 0, 0) for Si.[30] Thus an electron tunneling between the valence-band maximum at Γ and the conduction-band minimum must either emit or absorb a phonon of the appropriate wave vector in order to conserve crystal momentum. In tunneling across *p-n* junctions in heavily doped semiconductors, there are inflections in the I-V characteristic as the bias is increased to such values that the tunneling electrons can emit phonons of the appropriate wave vector.[31] LRT used electronic means to plot d^2I/dV^2 against V as these inflections then appear as peaks, considerably aiding their location. As their junctions were made by alloying to form the *p*-type material in an *n*-type wafer of the Ge-Si alloy, they adjusted the doping of the alloy so that the transitions took place towards the *n*-type side of the junctions rather than the nonuniform *p*-type side.

There is considerable evidence to indicate that the band structure of Ge-Si alloys varies linearly with concentration.[32] Both the optical[33,34] and transport[35] properties of the alloys indicate that the minimum conduction-band energy moves from L to along Δ as the concentration of Si exceeds about 0.15. As the minimum of the conduction band along Δ in Ge also lies at about (0.85, 0, 0), we assume that it also lies here in the alloys having Si concentrations greater than 0.15.

In a disordered crystal the wave vector is no longer expected to be a good quantum number. However, because it is possible to obtain the behavior of the optical energy gaps[36] in a clear manner in the Ge-Si alloys and because the band edges move almost linearly with concentration, it would seem a reasonable approximation to assume that the wave vector is a good quantum number for the electrons. The work of Soven[13] suggests the same conclusion. Thus in the assisted tunneling in the Ge-Si alloys, the tunneling electrons are measuring the vibrational response of the crystal at a given wave vector as a function of frequency (bias voltage). This wave vector equals $(2\pi/a)$ $(\frac{1}{2},\frac{1}{2},\frac{1}{2})$ for $0.85<c<1.0$ and $(2\pi/a)$ (0.85,0,0) for $0<c<0.85$, where c is the Ge concentration.

In order to compare theory and experiment we have solved (3.12) for $c=0.25$, 0.50, and 0.75 using the recent Si density of states of Dolling and Cowley.[37] So that the frequencies at $c=0$, 1 are approximately correct,

---

[26] M. E. Fisher, J. Math. Phys. **2**, 620 (1961).

[27] H. W. Verleur and A. S. Barker, Phys. Rev. **149**, 715 (1966).

[28] B. N. Brockhouse and P. K. Iyengar, Phys. Rev. **111**, 747 (1958).

[29] G. Dolling, in *Inelastic Scattering of Neutrons in Solids and Liquids* (International Atomic Energy Agency, Vienna, 1963), Vol. 2, p. 37.

[30] See for instance M. L. Cohen and T. K. Bergstresser, Phys. Rev. **141**, 789 (1966).

[31] For a review see E. O. Kane, J. Appl. Phys. **32**, 83 (1961).

[32] J. C. Phillips, Phys. Rev. **125**, 1931 (1962).

[33] E. R. Johnson and S. M. Christian, Phys. Rev. **95**, 560 (1954).

[34] R. Braunstein, A. R. Moore, and F. Herman, Phys. Rev. **109**, 695 (1958).

[35] M. Glicksman, Phys. Rev. **111**, 125 (1958).

[36] J. Tauc and A. Abraham, J. Phys. Chem. Solids **20**, 190 (1961).

[37] D. Dolling and R. A. Cowley, Proc. Phys. Soc. (London) **88**, 463 (1966).

we have scaled the Si frequencies by 0.58 to obtain those for Ge and have used $\epsilon = -1.970$ rather than $\epsilon = -1.582$ which would be appropriate to the actual change in mass. In the pure crystals at the appropriate values of **k**, there are modes at four different frequencies and these were read off Dolling's fitted dispersion curves for Si.[29] These frequencies are slightly lower than those of LRT which may be attributed to the fact that they made their measurements at helium temperatures whereas the neutron measurements were made at room temperatures.

The peaks in the spectral function are in the positions shown in Fig. 10, using the same notation as in Fig. 8. The peaks in the tunneling characteristics of LRT are indicated by crosses. Considering the approximations that have been made to effect this comparison there is seen to be fair agreement between theory and experiment for $c < 0.85$. As is expected from Fig. 8, the widths of the low-frequency peaks for the different values of $\omega_j(\mathbf{k})$ at $c = 0.50$ and 0.75 are such that these peaks cannot be resolved, helping to explain why LRT saw only one peak in this region. For $c = 0.75$, the open circles mark the maxima of smooth humps rather than peaks but can be considered to indicate the position of the upper region of the impurity band. This is just the situation in which our approximation is worst so that there is no real justification for believing the detailed predictions of the spectral functions. We found in Sec. 6 A that our density of states in the impurity band does not have the structure given by the machine calculations and, indubitably, our spectral function is similarly at fault.

We do not have the correct behavior for the upper longitudinal optic (LO) mode, and although there is some correlation between the relative magnitudes of the spectral function peaks and those of LRT, the former low-frequency peaks do not persist to such high Si concentrations as do the latter. This discrepancy may be partially attributable to differences in the electron-phonon interactions in Si and Ge. Unfortunately, it is not possible to make any statement about this relative interaction strength from the pure Ge and Si tunneling results. The four peaks for Ge are very sharp and of comparable magnitude whereas only the transverse acoustic (TA) and TO peaks are sharp for Si. However, as LRT suggest, this difference can be attributed to the comparable doping levels in the p and n regions for $c < 0.10$ with the resulting possibility that the tunneling transitions could also occur in the nonuniform regrown p region.

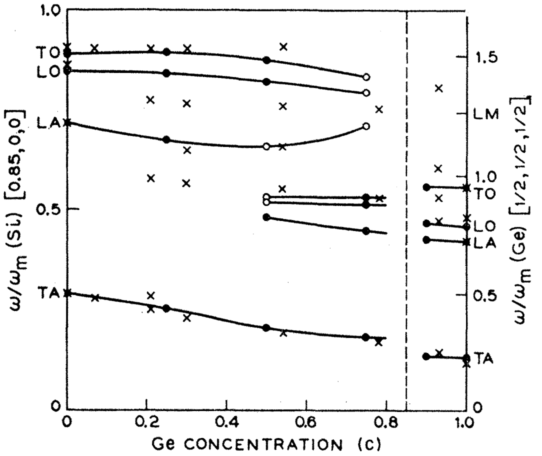

FIG. 10. Comparison between the spectral-function peaks for Ge-Si (same notation as Fig. 8) and the major peaks in the tunneling work of Logan, Rowell, and Trumbore (×).

For $c > 0.85$, there is no agreement between theory and experiment, and it is almost certain that the mass defect approximation has broken down. We observe that the TO mode has exceeded the maximum frequency for pure Ge by $c = 0.93$, whereas we know from Secs. 5 B and 6 A that this maximum frequency is reduced as light-mass defects are added. In this case the wave vector of the modes is on the zone boundary, and so they must be more sensitive to force-constant changes than modes whose wave vector is in the interior of the zone, as is the case for those observed when $c < 0.85$.

LRT interpreted their results by drawing a smooth line through four of their major peaks and used the model of Braunstein, Moore, and Herman[34] to suggest large deviations from random disorder in their alloys. From the above analysis, we conclude that their results can be understood in a qualitative manner using our theory so that it is not necessary to invoke such deviations, at least not of the magnitude that they suggest.

ACKNOWLEDGMENTS

The author wishes to thank M. Lax and P. Soven for many discussions on disordered systems. He also wishes to thank W. L. McMillan for useful conversations, R. A. Logan, J. M. Rowell, and F. A. Trumbore for access to their tunneling data, G. Dolling and R. A. Cowley for tabulations of their densities of states, and D. N. Payton for useful correspondence.